High Power Water Jet Guided Laser Cutting of SiC/SiC Ceramic Matrix Composite

Helen Elkington[*1], Sundar Marimuthu[1], and Bethan Smith[1]

[1]*The Manufacturing Technology Centre, Ansty Business Park, Coventry UK*
[*]*Corresponding author's e-mail:* helen.elkington@the-mtc.org

Laser processing is widely used in manufacturing metal alloy aerospace components. Over the last few years there has been an increased interest in exploiting silicon carbide (SiC) based ceramic matrix composite (CMC) materials for aero-engine components, as they possess superior thermo-mechanical properties compared to conventional alloys. However, laser processing of SiC CMCs is difficult due to their high melting temperatures, and differences present between the thermal and physical properties of the matrix and fibre. This paper investigates the basic characteristics of water jet guided laser (WJGL) cutting SiC/SiC, using a high power 532 nm Q-switched pulsed laser with an average power of 400 W. Experimental trials were performed to understand the effect of different process parameters on the cut quality and overall cutting speed. Cutting speed and pulse frequency were found to be key in determining cut quality and overall cutting speed on the WJGL. Average power also affected overall cutting speed. Due to the cooling nature of the water jet, the thermal damage typically associated with conventional laser processing was eliminated. However, heterogeneous removal of the material matrix and fibres was found to occur where fibres aligned parallel to the direction of the cut length, resulting in non-uniform kerf widths.

1. Introduction

The drive for developing more efficient, lightweight aero-engines has increased over the last decade. Composite materials, particularly ceramic matrix composites (CMC) play a key role in the development of these due to their superior properties.

Silicon carbide/silicon carbide (SiC/SiC) is an anisotropic high-temperature CMC which has been identified as an alternative to nickel superalloy for hot-section aero-engine components [1]. SiC/SiC offers a working temperature 200 K to 300 K higher than nickel superalloy, whilst maintaining a higher specific strength [2]. It also offers weight reductions of over 30% compared to current materials used within the aerospace industry and could improve fuel efficiency by 10% [3].

The hard and brittle nature of SiC/SiC means that machining SiC/SiC using traditional tool-based methods is difficult [3]. Consequently, non-conventional machining methods have been investigated for SiC/SiC machining. This includes laser processing which presents significant potential due to its high productivity, superior cut quality, and minimal tooling and consumable requirements.

Laser processing is exploited across manufacturing industries for numerous materials, including thick (>10 mm) materials [4]. However, most research performed using laser processing has focused on isotropic metals and alloys [4, 5], with anisotropic materials challenging due to the differences present in thermal properties throughout the material. Research which has investigated laser processing of anisotropic material largely concentrates on carbon fibre reinforced polymer composites [6], with considerably less literature available on laser processing of SiC/SiC.

Tuersley et al. [7] performed the first known investigation into SiC/SiC laser machining using a pulsed Nd:YAG laser to examine the effect of process parameters on cutting the material. More recent studies into laser machining of SiC/SiC have focused on short pulse and ultra-short pulse laser processing. By using a pulsed laser over a continuous wave laser, the heating duration and thus heat input into the material is reduced, thereby minimising thermal defects. In a study performed on SiC/SiC using a femtosecond laser, Zhai et al. [8] found that common defects associated with machining (fibre pull-out and chipping) and long pulse laser processing (heat affected zone and oxidation) could be eliminated.

Liu at al. [9] also used a femtosecond laser to investigate drilling of SiC/SiC, while Costil et al. [10] used a Nd:YAG nanosecond pulsed laser to investigate micromachining. Both studies give detailed surface characterisation of the SiC/SiC and observe a silicon oxide layer on the surface of the material following laser processing. This corresponds to other research which also found that SiC tended to produce silicon oxide when using a femtosecond laser [8, 11]. However, compared to nanosecond lasers, femtosecond lasers have been observed to be capable of producing significantly less silicon oxide [12]. Using a combination of experiments and numerical simulations, Chen et al. [13], investigated the ablation of SiC/SiC. They found the ablation products to predominantly consist of amorphous SiO_2 and recrystallized 3CSiC.

Water jet guided laser (WJGL) processing offers an alternative to short and ultra-short pulsed laser systems for minimising thermal defects. The process uses a pressurised water jet to guide a laser beam through total internal reflec-

tion (at the air/water interface) to the laser irradiation zone at the workpiece, as shown in Fig.1.

WJGL processing presents many benefits over conventional laser processing. The continuous application of water ensures cooling during processing, significantly reducing the negative effects associated with laser heating, resulting in negligible thermal damage. The cylindrical beam created by the water jet produces parallel kerfs – minimising taper. The working distance of the laser beam is extended by the water jet, allowing the WJGL head to remain at the same distance from the workpiece surface during processing.
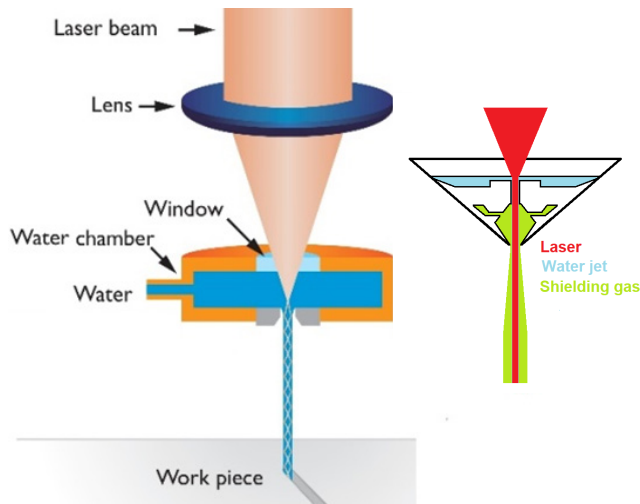

Fig.1 Schematic of the water jet guided laser.

WJGL processing has been evaluated for a range of applications. Marimuthu et al. [14] found WJGL drilling to be capable of producing acute angular holes through a thermal barrier coated nickel alloy, with no spatter, recast layer, or delamination observed. Damage free hole drilling through aluminium metal matrix composites has also been demonstrated [15]. Research has also been carried out into WJGL machining of ultra-hard materials, such as diamonds [16] and semiconductors [17].

Current research into WJGL machining of SiC/SiC is limited. A comparison using three laser systems to cut SiC/SiC was carried out by Marimuthu et al. [18]. They observed a continuous wave laser to be both quicker and produce a better cut quality than a millisecond pulsed laser, but found WJGL cutting could offer even better quality.

By introducing a novel coaxial helical gas atmosphere to surround the water jet during processing, Cheng et al. [19] could extend the stable length of the water jet. In doing this the ablation volume could be increased. They also found that using argon to shield the water jet during processing promotes ablation efficiency more significantly than compressed air or nitrogen. In another study, Cheng et al. [20] developed a finite element method model to analyse the distribution and evolution of the temperature field during WJGL machining of SiC/SiC CMC. They observed the WJGL to effectively limit the thermal damage induced by the laser, finding it capable of producing a surface morphology containing no recast layer, heat-affected zone, delamination, or pulling-out of SiC fibres. This indicates that this technology could provide a method by which to machine CMCs to a high-quality.

Despite the widespread advantages of CMCs, there is little public information available on the effects of laser parameters on cutting these materials. This research aims to investigate and evaluate the performance of using a high power WJGL system for cutting SiC/SiC CMC.

2. Methods and materials

This work was performed using a 5-axis Synova laser-microjet LCS 305 system, fitted with a 532 nm Q-switched diode pumped solid state laser. This has a maximum average power of 400 W and operates in nanosecond pulse duration. The laser beam is focussed into a ~70 µm diameter water jet, which exits the nozzle at a pressure requested by the system user.

Using this system, 25 mm length linear cuts were made through 2 mm thick SiC/SiC. A bi-directional scan strategy was used, with the distance from the cutting head to the workpiece kept constant at 10 mm. For each cut, the number of passes required to achieve total breakthrough was recorded.

As the WJGL process is a relatively new technology, the effect of the process parameters on experimental results is not well understood. Thus, a systematic investigation based on changing one parameter at a time was performed. This is experimentally expensive, however provides quantifiable evidence on the effect of each individual laser parameter on the experimental outcome. This will enable future work focusing on the interaction effect between the process parameters.

The process parameters varied in this study were shielding gas flow rate, scanning speed, pulse frequency, and average power. Parameter ranges were selected based on initial experimental trials. Table 1 shows each set of experimental parameters. Water jet pressure was kept constant at 300 bar, and pulse gap at 440 ns.

Cut entrance and exit profiles were analysed using a Dinolite microscope and a TM 3000 Tabletop scanning electron microscope (SEM). Metallurgical preparation of the cut cross-sections was conducted as per ASTM E3-11 [21]. A Keyence microscope was used to analyse the cross-sections, examine wall regularity, and measure the process affected zone (PAZ). Internal sections of the cut wall were analysed using the SEM.

Table 1 Experimental parameters and pulse durations.

	Frequency	Pulse duration	Average power	Scan speed	Gas flow rate
	kHz	ns	W	mm/s	L/min
1	10	309	131	10	3.5
2	14	365	131	10	3.5
3	18	420	131	10	3.5
4	22	470	132	10	3.5
5	26	508	131	10	3.5
6	30	543	131	10	3.5
7	34	560	131	10	3.5
8	10	232	200	10	3.5
9	18	345	202	10	3.5

10	22	389	201	10	3.5
11	26	421	199	10	3.5
12	30	479	164	10	3.5
13	34	477	191	10	3.5
14	18	276	252	10	3.5
15	22	311	252	10	3.5
16	26	343	250	10	3.5
17	30	374	246	10	3.5
18	34	403	242	10	3.5
19	38	428	242	10	3.5
20	30	660	92	10	3.5
21	30	660	92	40	3.5
22	30	660	92	70	3.5
23	30	660	92	100	3.5
24	22	615	92	70	3.5
25	14	570	92	70	3.5
26	10	513	92	70	3.5
27	6	455	92	70	3.5
28	22	615	92	70	3.5
29	22	615	92	70	3.5
30	22	615	92	70	3.0
31	22	615	92	70	2.5
32	22	615	92	70	2.0
33	22	615	92	70	3.5
34	26	638	92	70	3.5
35	30	660	92	70	3.5
36	34	678	92	70	3.5
37	38	693	92	70	3.5
38	22	615	92	70	3.5
39	22	615	92	70	3.5
40	22	615	92	70	3.5
41	22	615	92	70	3.5
42	22	615	92	70	3.5

3. Results and Discussion

Fig. 2(a) shows that heterogenous removal of the material matrix and fibres occurred where fibres aligned parallel to the cut length, resulting in non-uniform kerf widths through the material. This region corresponds to the area which has been affected during processing, providing a measure of the PAZ. No evidence of melting was observed. Cuts showed minimal taper, due to the water jet guiding the laser beam and keeping it at a constant diameter through the material during cutting.

Edge chipping was observed around the entrances and exits of cuts, this is shown in Fig. 2(b). This edge chipping occurs mostly on fibres which are perpendicular to the cut direction and relates to the material removal mechanism. For an isotropic material, the material removal mechanism is based predominantly on melting and melt ejection [14]. During WJGL machining, the SiC fibres, especially the fibres which are perpendicular to the laser scan direction are removed not just due to melting/melt ejection, but predominantly due to fracture.

The thermal conductivity of the fibre is significantly higher along the fibre direction, resulting in a change of mechanical properties (due to high temperature and thermal expansion) beyond the laser-material interaction zone. When the water jet interacts with the highly stressed fibre, the axial force induced by the high pressure of the jet causes the fibres to fracture. This results in the edge chipping observable around the cut entrances and exits.

Examination of the internal cut edges found the cross section of the fibres which aligned perpendicular to the cut length to have sheared, whilst the fibres which aligned parallel to the cut length displayed a non-uniform jagged appearance. This is demonstrated in Fig. 3.
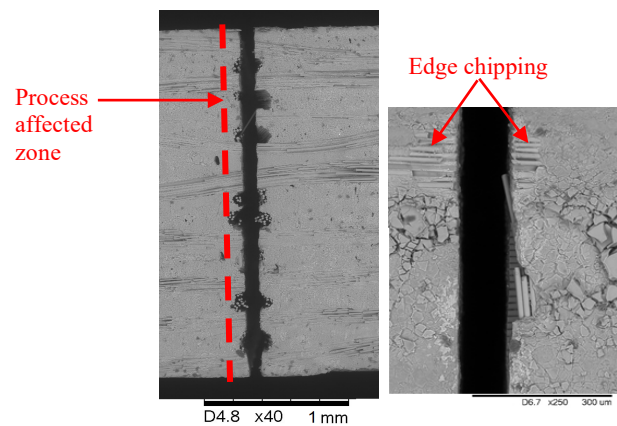

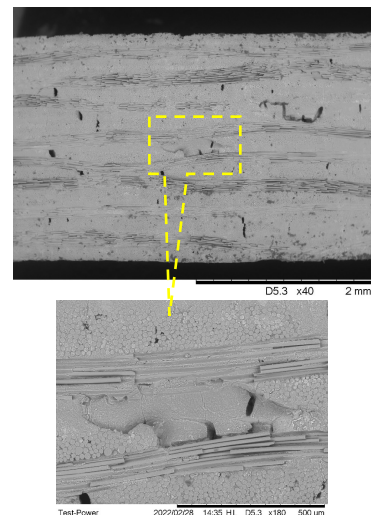**Fig. 2** SEM image of a cut cross section (a) and an entrance (b).

Fig. 3 SEM images of the internal cut side

The PAZ forms due to the heat input into the fibres and matrix adjacent to the cut during processing. The mismatch in thermal expansion between the fibres and matrix causes de-bonding between them. For the fibres which are perpendicular to the cut length, only a small region of a fibre and its surrounding matrix is subject to this. As these fibres extend into the bulk of the material, they are better supported and detained by their surrounding material. However, for the fibres which are parallel to the cut length, longer lengths of individual fibres and their surrounding matrix is

affected. This results in greater de-bonding between a fibre and the matrix, thus enables sections of the matrix to be more easily removed. This leaves the fibres exposed, as shown in Fig. 4, and increases the fibres susceptibility to shearing by the force of the water jet.
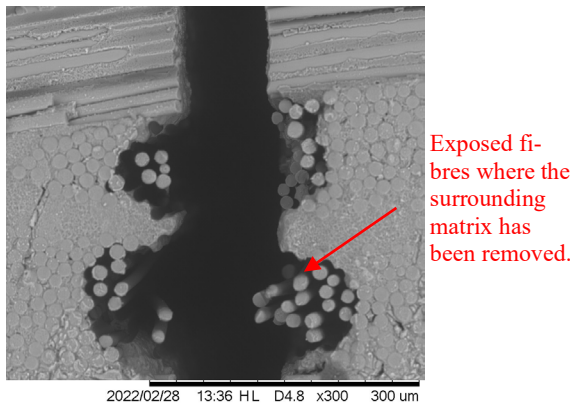

Fig. 4 SEM image of a cut cross section, containing exposed fibres which are parallel to the cut length.

3.1 Number of Passes

By varying the number of passes whilst keeping other parameters constant, the cut progression and PAZ development could be examined. The cross section of these cuts is shown in Fig. 5. Fig. 6 shows that material removal occurred linearly from 4 passes, whilst the PAZ increased as the number of passes progressed. This is due to the increased exposure to the laser increasing the thermal input, whilst the increased exposure to the high pressure of the water jet may increase the opportunity for process affected material to be removed.
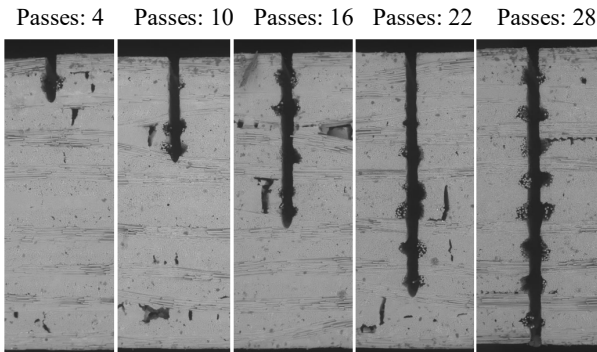

Fig. 5 Cross sections of cuts under increasing number of passes (22 kHz, 92 W, 3.5 L/min, 70 mm/s).
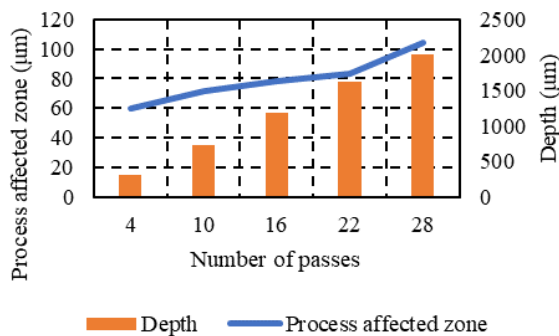

Fig. 6 Effect of number of passes on PAZ and cut depth.

3.2 Gas Flow Rate

Helium was used at the shielding gas to protect the water jet from interference as it guides the laser beam.

Optical examination found the entrance cut profile to improve as gas flow rate was increased from 2.0 L/min to 3.5 L/min (Fig. 7). The surface discolouration which appears around the cut entrance is significantly reduced as the gas flow rate was increased to 3.5 L/min. This surface discolouration occurs due to residual heating of the material as the cut propagates inside the material. At the lower gas flow rate (2.0 L/min), the laminarity of the jet is disturbed within the kerf after a depth of few 100 microns, resulting in beam divergence and heating of the material, without controlled material removal. Whereas with a sufficiently high gas flow rate, the laminarity of the jet is maintained with the kerf till the material is fully cut, resulting in minimal residual heating, and producing a cut without surface discolouration. Thus, a better entrance quality is observed at higher gas flow rates.

Gas flow rate was not found to affect through-cut quality, cut exit profile, or overall cutting speed. This lack of effect on other variables is attributed to the shielding gas being deflected from the workpiece surface upon reaching it. This means that whilst increasing gas flow rate can ensure a good quality entrance profile, it is not critical in determining through-cut quality.
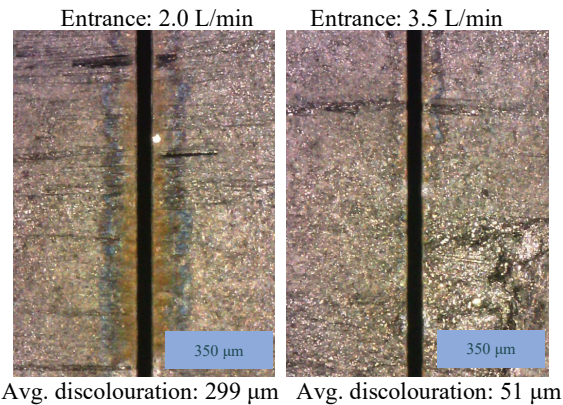

Fig. 7 Optical micrographs of the cut entrances at 2.0 L/min and 3.5 L/min (22 kHz, 92 W, 70 mm/s).

3.3 Scanning Speed

As Fig. 8 shows, increasing the scanning speed increased the overall cutting speed. With conventional laser cutting processes, a slower scan speed is typically associated with increased overall cutting speeds due to the increased laser-material interaction time. However this is not the case for the WJGL. During WJGL cutting, the water jet becomes turbulent at the base of the kerf, interfering with, and disturbing the water jet. This disrupts the interaction which occurs between the laser and the material, reducing the efficiency of the WJGL in removing material. This turbulence is increased at slower scan speeds due to the greater volume of water reaching the kerf base (and ejected upwards) per unit time.

Whereas by increasing the scanning speed, the volume of water impacting the base of the kerf per unit time is reduced, reducing the turbulence which the water jet experiences. This reduction in turbulence allows ideal

interaction between the laser and the material, improving material removal efficiency, thus acting to increase the overall cutting speed. Both the PAZ and the kerf width decreased with increasing scanning speed. This occurs due to the reduced interaction time between the WJGL and the material, which reduces the energy per unit area.
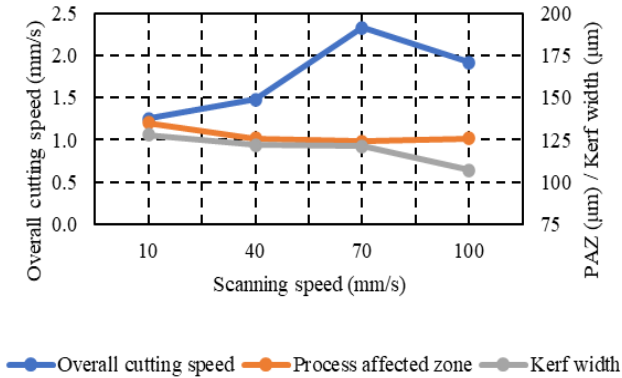

Fig. 8 Effect of scanning speed on overall cutting speed, PAZ, and kerf width (30 kHz, 92 W, 3.5 L/min).

3.4 Pulse Frequency

By altering the pulse frequency, both pulse energy and peak power are changed. As Fig. 9 and Fig. 10 show, increasing the pulse frequency from 6 kHz (16.3 mJ; 35.7 kW) to 22 kHz (4.4 mJ; 7.2 kW) increased overall cutting speed, and decreased the kerf width and PAZ. However, further increases in pulse frequency decreased overall cutting speed, and increased the kerf width and PAZ.

Higher pulse energy and peak powers, thus lower pulse frequencies, are expected to increase overall cutting speed through increasing material removal. However, this was not observed between 6 kHz and 22 kHz. This lower overall cutting speed corresponded to an increased kerf width at lower pulse frequencies, highlighting that increased material removal has occurred at the kerf edges rather than downward through the cut. Thus, despite the lower pulse frequency increasing the volume of material removed, it has not increased the cutting speed.
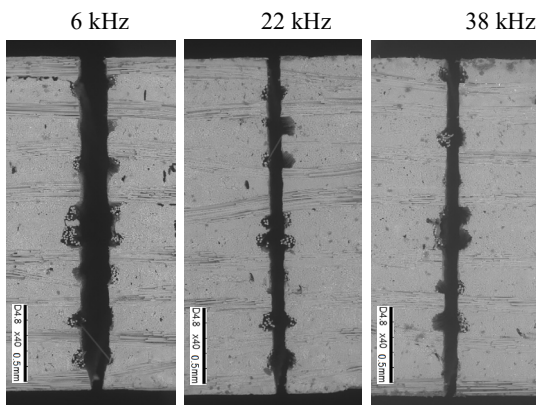

Fig. 9 SEM images of cross sections at 6 kHz (16.3 mJ; 35.7 kW), 22 kHz (4.4 mJ; 7.2 kW), and 38 kHz (3.2 mJ; 4.9 kW). (92 W, 70 mm/s, 3.5 L/min).
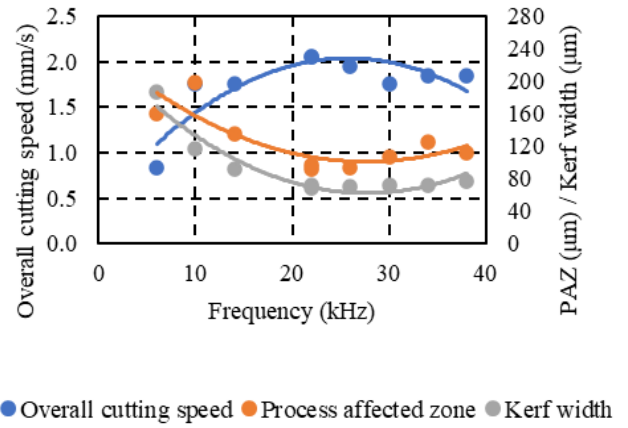

Fig. 10 Effect of frequency on overall cutting speed, PAZ, and kerf width (92 W, 70 mm/s, 3.5 L/min).

3.5 Average Power

Increasing average power from 92 W (3.3 mJ; 4.9 kW) to 252 W (15 mJ; 54.2 kW) at a scan speed of 10 mm/s and shielding gas flow rate of 3.5 L/min increased the overall cutting speed (Fig. 11). This is attributed to the increased peak power that occurs when average power is increased through changing the pulse energy, whilst maintaining a constant frequency. The increased peak power promotes material vaporisation and ejection, increasing the overall cutting speed. As this also increases the thermal input into the material, a larger PAZ would be expected at higher average powers. However, no correlation was observed between average power and the PAZ, indicating that at below 252 W, average power is not a dominating factor in determining cut quality. This also indicates that it could be possible to use lasers of higher average power without negatively affecting the cut quality. Fig. 12 shows cross sections of cuts at 92 W and 252 W.
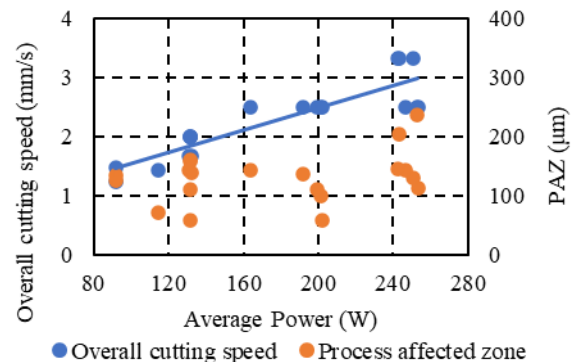

Fig. 11 Effect of average power on overall cutting speed and PAZ (70 mm/s, 3.5 L/min).
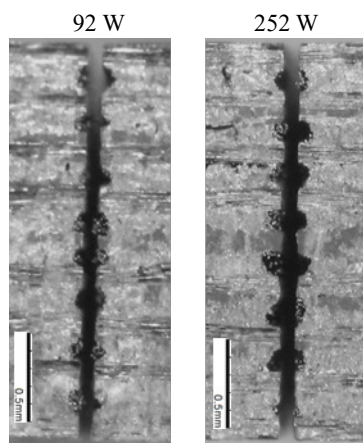
92 W   252 W

Fig. 12 Optical micrographs of cross sections at 92 W (3.3 mJ; 4.9 kW) and 252 W (15 mJ; 54.2 kW) (10 mm/s, 3.5 L/min).

4. Summary

In this paper, a systemic investigation was performed to understand the characteristic of WJGL cutting of SiC/SiC CMC. The findings can be summarised as follows:

(1) Scan speed and pulse frequency are key in determining the cut quality and overall cutting speed, with average power also affecting overall cutting speed.

(2) Cuts can be produced which display no taper, indicating that the WJGL process could be used to process thicker SiC/SiC, or other advanced CMC materials.

(3) The WJGL can eliminate the thermal damage typically associated with conventional laser processing at average powers up to 252 W – the maximum used within this work.

(4) Although the WJGL is beneficial for reducing the thermal damage typically associated with conventional laser processing. The high pressure of the water jet combined with the thermal input of the laser causes grooves where excess material has been removed down the cut kerf.

Future work will focus on exploring how the PAZ induced by the combined effect of the lasers thermal input and water jet pressure can be reduced or eliminated.

References
[1] H. Ohnabe, S. Masaki, M. Onozuka, K. Miyahara, and T. Sasa: Compos. Part A Appl. Sci. Manuf., 30, (1999) 480.
[2] D. Marshall and B. Cox: Annu. Rev. Mater. Sci., 38, (2008) 425.
[3] Q. An, J. Chen, W. Ming, and M. Chen. Chinese J. Aeronaut., 34, (2020) 540.
[4] S. Marimuthu, A. Nath, D. Bandyopadhyay, S. Chaudhuri, P. Dey, and D. Misra: Int. J. Adv. Manuf. Tech., 40, (2008) 865.
[5] A. Sharma and V. Yadava: Opt. Laser Technol., 98, (2018) 264.
[6] M. El-Hofy and H. El-Hofy: Int. J. Adv. Manuf. Technol., 101, (2019) 2965.
[7] I. Tuersley, T. Hoult, and I. Pashby: Part 1. J. Mater. Sci., 33, (1998) 955.
[8] Z. Zhai, C. Wei, Y. Zhang, Y. Cui, and Q. Zeng: Appl. Surf. Sci., 502, (2020) 144131.
[9] Y. Liu, R. Zhang, W. Li, J. Wang, X. Yang, L. Cheng and L. Zhang: Int. J. Adv. Manuf. Technol., 96, (2018) 1795.
[10] S. Costil, S. Lukat, C. Langlade, and C. Coddet: App. Surf. Sci., 255, (2008) 2425.
[11] Z. Zhai, Y. Zhang, Y. Cui, Y. Zhang, and Q. Zeng. Optics., 224, (2020) 165719.
[12] P. Rudolph, K. Brzezinka, R. Wasche, and W. Kautek: App. Surf. Sci., 208, (2003) 285.
[13] J. Chen, Q. An, W. Ming, and M. Chen: J. Eur. Ceram. Soc., 41, (2021) 5835.
[14] S. Marimuthu and B. Smith: Int. J. Adv. Manuf. Technol., 113, (2021) 177.
[15] S. Marimuthu, J. Dunleavey, Y. Liu, A. Kiely, and M. Antar: J. Compos. Mater., 53, (2019) 3787.
[16] G. Shi, D. Han, S. Wang, and K. Zhu: AER., 146, (2018) 195.
[17] O. Sibailly and B. Richerzhagen: Proc SPIE, Col. 5339, (2004) 529038.
[18] S. Marimuthu, N. Burtt, H. Elkington, and B. Smith: Advanced Engineering of Materials Through Lasers. AMRT, (Publisher, Springer, 2022) p.55.
[19] B. Cheng, D. Ye, L. Yuan, L. Jingyi, X. Junjie, L. Qiang, and Y. Lijun: J. Mater. Process. Tech., 293, (2021) 117067.
[20] B. Cheng, D. Ye, L. Yuan, and L. Yang: Appl. Sci., 12, (2022) 1214.
[21] ASTM International Standard E3-11 (2012).